A statistical method to model non-stationarity in precipitation records changes

Paula Gonzalez, Philippe Naveau, Soulivanh Thao, Julien Worms

A statistical method to model non-stationarity in precipitation records changes

Paula Gonzalez[1], Philippe Naveau[1], Soulivanh Thao[1], and Julien Worms[2]

[1]Université Paris-Saclay, UVSQ, Laboratoire des Sciences du Climat et de l'Environnement, LSCE/IPSL/ESTIMR, CNRS-CEA, Gif-sur-Yvette, France.
[2]Université Paris Saclay, UVSQ, Laboratoire de Mathématiques de Versailles, CNRS, Versailles, France.

Key Points:

- This work proposes a simple definition of non-stationary records and offers a method to assess the likelihood of record event changes.
- We analyze annual maxima of daily precipitation, whose statistical features strongly depart from a Gaussian probability distribution.
- IPSL-CM6A-LR climate model highlights that by 2023 signals of rainfall yearly maxima decadal records have emerged on the half of the globe.

Corresponding author: Paula Gonzalez, `paula.gonzalez@lsce.ipsl.fr`

Abstract

In the context of climate change, assessing how likely a particular change or event was caused by human influence is important for mitigation and adaptation policies. In this work we propose an extreme event attribution (EEA) methodology to analyze yearly maxima records, key indicators of climate change that spark off media attention and research in the EEA community. Although they deserve a specific statistical treatment, algorithms tailored to record analysis are lacking. This is particularly true in a non-stationarity context. This work aims at filling this methodological gap by focusing on records in transient climate simulations. We apply our methodology to study records of yearly maxima of daily precipitation issued from the numerical climate model IPSL-CM6A-LR. Illustrating our approach with decadal records, we detect in 2023 a clear human induced signal in half the globe, with probability mostly increasing, but decreasing in the south and north Atlantic oceans.

Plain Language Summary

The increase of frequency and strength of climate extremes raises the interest in quantifying the extent to which these changes are influenced by climate change. In this work we propose an Extreme Event Attribution (EEA) methodology allowing us to assess whether climate records are attributable to climate change. Records have been typically studied by considering climate unvarying in some time span, despite the fact that climate is constantly changing. This work aims at filling this methodological gap by focusing on records in time-varying climate simulations. We apply our methodology to study records of yearly maxima of daily precipitation issued from the latest version of the Institute Pierre Simon Laplace climate model. Illustrating our approach with decadal records, we detect in 2023 a clear human induced signal in almost half of the globe. Even though decadal record probability mostly increases, we observe a decrease of record probability in the south and north Atlantic oceans.

1 Introduction

In its recent media release on January 23rd 2023, the European Copernicus program highlighted that *2022 was a year of climate extremes, with record-high temperatures and rising concentrations of greenhouse gases.* This statement underlines the current interest in records changes and records breaking. This can be explained by their high societal and economic impacts, the question of mitigation and the attribution to anthropogenic forcings. Assessing how likely a particular extreme event has been caused by human influence has been an active field of research (IPCC, 2014). Changes in various climate events have been well documented (Gulev et al., 2021), for example concerning the frequency and intensity of extreme precipitation at continental to global scales (Dong et al., 2021; Alexander, 2016).

To attribute changes in any extreme climate variable, the field of extreme event attribution (EEA) (see, e.g., Stott et al., 2016; Naveau et al., 2020) specifically aims at comparing the probability of the same extreme climate event within two different realities: a *factual* world that mimics the conditions observed around the time of the event (i.e, a world that contains the effect of human influence on climate) and a *counterfactual* world, in which anthropogenic emissions have never occurred (Angélil et al., 2017). This design of experiment can only be tested via numerical climate models as a world without anthropogenic forcing does not exist (Hegerl & Zwiers, 2011). This numerical setup seeks to address the following question: can we attribute the change of likelihood of a particular extreme event to the difference between the factual and counterfactual worlds? Mathematically, most EEA studies compare the following two probabilities of exceeding some

high threshold u for a given year t;

$$p_{0,u}(t) = P(X_t > u) \quad \text{and} \quad p_{1,u}(t) = P(Z_t > u), \tag{1}$$

where the notations X_t and Z_t represent the same real-valued variable of interest (e.g., annual maxima of daily precipitation in our application) but X_t corresponds to its counterfactual version while Z_t denotes its factual one. The temporal index t will correspond to the years from 1850 to 2100 in our application, see Section 3. The choice of the threshold u that defines the extreme event is usually delicate and depends on the case study at hand. $1-\frac{p_{1,u}(t)}{p_{0,u}(t)}$ has been called the fraction of attributable risk by Stott et al. (2016). This type of ratio can be interpreted within Pearl's counterfactual theory of causality (Hannart et al., 2016; Hannart & Naveau, 2018). By leveraging multivariate extreme value theory (EVT), this relative ratio can be optimized to highlight causality (see, e.g., Kiriliouk & Naveau, 2020).

It is important to notice that, given a fixed u and a year of interest t, the probabilities defined by (1) do not directly provide relevant information concerning records. In this article we provide a methodology to analyze record events in a non-stationary context. The meaning of *records* is not based on a fixed threshold. Instead, it is rooted in the comparison between the current value and past observations. For example, the statement that 2016 was the warmest global temperature on record can only be understood with respect to a reference period, here since the moment when reliable instrumental measurements were available. Mathematically, the probability of being a record with respect to a given period $\Re$ can be generically defined as

$$P(Y > \max(X_t : t \in \Re)), \tag{2}$$

where the event $\{Y > \max(X_t : t \in \Re)\}$ means that the value Y is larger than any value from the sample X obtained during the reference period $\Re$. As highlighted previously, EEA is rooted in the comparison between factual and counterfactual data, the later being considered as the baseline. Regarding this yardstick, it is natural to wonder what is the probability of observing a record in the counterfactual world, i.e. taking $Y = X_{t+1}$ in (2) with respect to a given reference period $\Re = \{1, \ldots, T\}$. A similar but more complex question is to estimate the probability that the *factual* observation at time $T+1$, i.e. taking $Y = Z_{t+1}$ in (2), would have been a record in the *counterfactual* world. This leads to our two new definitions of record probabilities

$$\begin{aligned} p_{0,r}(t) &:= P(X_t > \max(X_{t-1}, ..., X_{t-r+1})), \\ p_{1,r}(t) &:= P(Z_t > \max(X_{t-1}, ..., X_{t-r+1})), \end{aligned} \tag{3}$$

where, given the $r-1$ counterfactual observations before the year t, $p_{0,r}(t)$ represents the probability of the counterfactual value being the largest at time t, and $p_{1,r}(t)$ is the same quantity but when the last value comes from the factual world. This setup is similar to return level computations. For example, the 100-year return period in risk analysis is given to a risk manager and the task is to estimate the corresponding 100-year return level from a sample of data. The record length r can be arbitrarily set in our study. The simplest form of this definition arises when setting $r = 2$. This special case was studied in (Naveau & Thao, 2022). It comes down to comparing the central part of the factual and counterfactual distributions with one statistic. In this paper, our goal is to estimate $p_{1,r}(t)$ for any positive integers r. We would like to highlight that it is possible to find two factual worlds, Z_t and Z_t^* such that $P(Z_t > X_{t-1}) = P(Z_t^* > X_{t-1})$ and $P(Z_t > \max(X_{t-1}, X_{t-2})) \neq P(Z_t^* > \max(X_{t-1}, X_{t-2}))$. So checking $p_{1,2}(t)$ is not sufficient to capture other changes in r, (see example in the Supplementary material, section 1.

To understand the difference between $p_{0,r}(t)$ and $p_{1,r}(t)$ in a non-stationarity context, we compare them in Figure 1 for $r = 50$ years and two different years, $t = 1950$

in panel (a) and $t = 2050$ in panel (b). The sequence of blue-colored dots indicates a simulated example of a counterfactual time series X_t with t varying from 1850 to 2100, while the sequence of red-colored points represents a factual trajectory. The upper panel highlights the year $t = 1950$ with the grey vertical band enlighting its associated reference period from 1900 to 1949. The probability $p_{1,50}(1950)$ assesses how often the red diamond of the year 1950 could have been above the maximum of the blue solid dots. During the time window 1900−1950, the effect of the anthropogenic forcing is not very apparent in this example, and $p_{1,50}(1950)$ should be close to the value of $p_{0,50}(1950)$. In contrast, observing a factual record in 2050 with respect to the counterfactual world of 2000−2050 should be much more probable, i.e. $p_{1,50}(2050)$ is much greater than $p_{0,50}(1950)$ in this artificial example. The bottom panel (b) highlights this phenomenon as the non-stationarity of Z_t increases the likelihood of the red diamond of 2050 to be above the largest value of X_t with t spanning 2000−2050. In this simulated example, this can be clearly seen with the probability density functions (pdf) displayed on the right side of Figure 1. The red pdf in panel (a) that corresponds to the pdf of Z_t for year $t = 1950$ has been switched up in year $t = 2050$. This non-stationarity in the factual world explains the change in 50-year records and highlights the necessity of interpreting records with respect to a chosen time window.

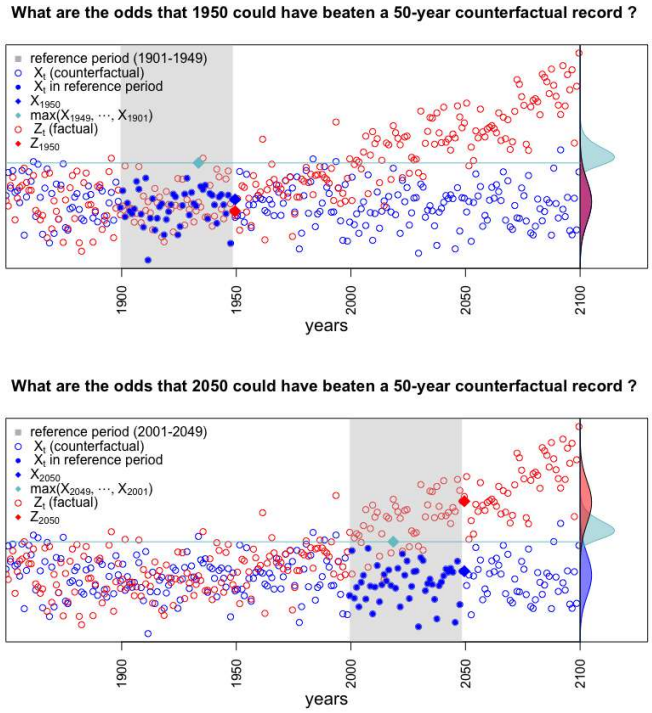

Figure 1. Schematic example to interpret the 50-year record probabilities (i.e. $r = 50$ in Equation (3)) in a non-stationary context. The upper panel highlights the year $t = 1950$ and the lower panel, the year $t = 2050$. The blue and red colors represent a simulated counterfactual trajectory, X_t, and a factual one, Z_t, respectively. The solid blue dots correspond to $(X_{t-1}, ...X_{t-49})$. On the right side of the plot, the probability density functions of Z_t, X_t and $\max(X_{t-1}, ...X_{t-49})$ are displayed in red, blue and light blue, respectively.

As already pointed out, one advantage of prefering records over exceedances is that there is no need to choose a threshold u like in (1), but this is not the only one. Record

analysis relies on their relative nature. For each climate model the reference value of comparison is derived from the model's own outputs, allowing us to easily compare the results. In some instances, this allows to bypass the bias correction steps in multi-model error analysis (Naveau & Thao, 2022). More importantly, the interpretation of $p_{0,r}(t)$ corresponds to the classical understanding of records for the general public. The expression of $p_{0,r}(t)$ is also very simple

$$p_{0,r}(t) = \frac{1}{r}, \quad \text{for all years } t \text{ in a reference period of length } r, \tag{4}$$

under the assumption of exchangeability in the counterfactual world (Chow & Teicher, 2003). For example, yearly maxima of daily precipitation, due to their high temporal variability at the yearly scale, can be considered independent and identically distributed (iid) at the yearly scale in the counterfactual world, and therefore exchangeable.

(4) 2 For illustration purposes, Figure 2,panel (a) shows how Equation (4) can be derived from the exchangeability assumption. It displays the bivariate pdf of exchangeable max-stable variables (X_t, X_{t-1}) (see Supplementary material, section 2) (Beirlant et al., 2005; Coles, 2001). Since X_t and X_{t-1} are exchangeable, $P(X_t > X_{t-1}) = P(X_{t-1} > X_t)$, and consequently $p_{0,2}(t) = 1/2$.

This can be visually understood by noticing the symmetric nature of panel (a) around the diagonal. The zone highlighted in red represent the event $\{X_t > X_{t-1}\}$, which under the exchangeability assumption, represents half of the mass of the pdf. In contrast, (b) focuses on the couple (Z_t, X_{t-1}) for $t = 2050$, which represents the case of $r = 2$ in the factual world, here $p_{1,2}(t) = P(Z_t > X_{t-1}) = .71$. We notice that the bivariate pdf is no longer symetric with respect to the $\{Z_t = X_{t-1}\}$ line. The event $\{Z_t > X_{t-1}\}$, represented in red contains more mass than in panel (a), meaning that the probability of this event is higher. Then, for $r = 2$ exchangeability of the counterfactual world allow us to do attribution by comparing $p_{1,2}(t)$ to $1/2$. For $r = 3$, exchangeability provides $P(X_t > \max(X_{t-1}, X_{t-2})) = P(X_{t-1} > \max(X_t, X_{t-2})) = P(X_{t-2} > \max(X_t, X_{t-1}))$, and leads to $p_{0,3}(t) = 1/3$. This argument can be repeated for any r in an exchangeable counterfactual world. 2 In panel (c), we now consider the decadal records probability $p_{0,10}$ by looking at a bivariate density of the vector $(X_t, \max(X_{t-1}, ..., X_{t-9}))$. The zone in red represents the event $X_t > \max(X_{t-1}, ..., X_{t-9})$ and contains $1/10$ of the mass of the bivariate pdf. In contrast, panel (d) shows $p_{1,10}(t) = .18$ for $t = 2050$ as probability for the factual value Z_t to become a decadal record with respect to $\max(X_{t-1}, ..., X_{t-9})$. Therefrom, the main problem we would like to address in this work is how to efficiently and rapidly estimate $p_{1,r}(t)$ for any given year t and for any given record length r in a non-stationary context.

This article is organized as follows. In Section 2, we propose a new methodology that handles non-stationary situations when attributing records. In Section 3, we apply this transient record approach to analyze yearly maxima of daily precipitation issued from climate model IPSL-CM6A-LR from the CMIP6 inter-comparison projet. Finally, in Section 4, we summarize the added value of this methodology and discuss the results.

2 Inference of non-stationary record probabilities

Our inference goal is to estimate $p_{1,r}(t)$ for any record period length r. This means that r can even be larger than the length of time series under study, i.e. our approach should be able to extrapolate beyond the largest record ever observed in either the factual or counterfactual worlds. Similarly to the computation of high return levels in hydrology (Katz et al., 2002), the developed approach here is unconditional in the sense that there is not need to observe a realization of the event of interest (a record) to compute its probability of occurrence. Performing such unconditional extrapolation implies that a parametric model needs to be imposed, theoretically justified and tested.

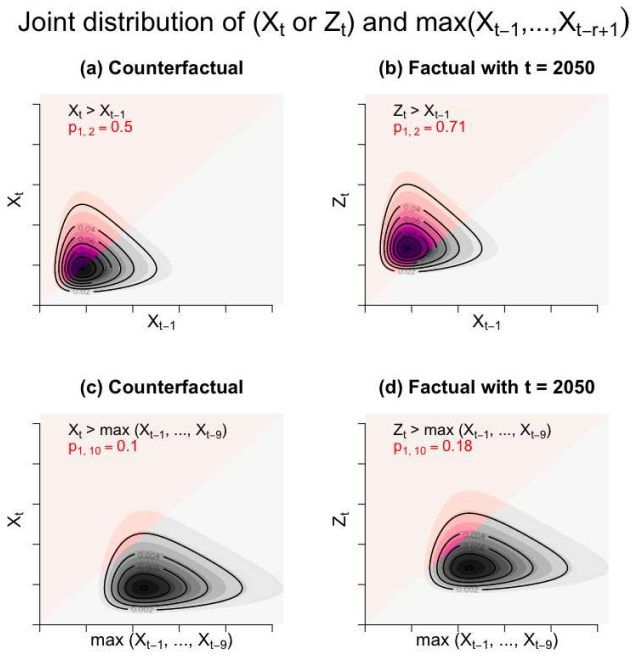

Figure 2. Joint distribution of X_t and $\max(X_{t-1}, ...X_{t-r+1})$ and of Z_t and $\max(X_{t-1}, ...X_{t-r+1})$ in 2050. (a) and (b) illustrate the case $r = 2$, where our probability of interest is $p_{1,2}(t) = P(Z_t > X_{t-1})$,(c) and (d) illustrate the case $r = 10$, where our probability of interest is $p_{1,10}(t) = P(Z_t > \max(X_{t-1}, ...X_{t-9}))$, the reddish zones represent our events of interest and the intersection between these zones and the pdf its probability.

The variable of interest in our study corresponds to annual block maxima (of daily rainfall). According to EVT, the classical three-parameter extreme generalized distribution (GEV) (Coles, 2001; Beirlant et al., 2005) should represent a mathematically sound distribution for such variables. Within this framework, one modeling possibility would be to fit a three parameter GEV to the counterfactual time series, and a different three parameter GEV to the factual temporal sequence. By noticing that records are relative quantities, Worms and Naveau (2022) showed, that under the conditions stated in their Lemma 1, the estimation of the six GEV parameters can be reduced to inferring only the two parameters of the following Weibull random variable defined as

$$W_t = -\log G(Z_t) \sim \text{Weibull}\,(k_t, \lambda_t), \tag{5}$$

where $G(x) = P(X_t \leq x)$ corresponds to the cumulative distribution function of X_t.

Weibull (k_t, λ_t) denotes a Weibull distribution, with positive parameters k_t and λ_t, that can be defined by its Laplace transform

$$\mathrm{E}\left[\exp(-uW_t)\right] = \int_0^\infty e^{-ux} \frac{k_t}{\lambda_t} \left(\frac{x}{\lambda_t}\right)^{k_t - 1} e^{-(x/\lambda_t)^{k_t}}\, dx.$$

A bivariate vector (X_t, Z_t) satisfying (5) is said to belong to the so-called *W-class*. Under this class, we can make the link between the computation of $p_{1,r}(t)$ and the Weibull Laplace transform.

As previously mentioned, in our application the sequence $(X_1, ..., X_t)$ can be assumed independent, and consequently

$$p_{1,r}(t) \quad = \quad \mathrm{E}(\exp(-(r-1)W_t)),$$

whenever Z_t is independent of $(X_1, \ldots, X_{t-1})$. This info and a reparametrization of the Laplace integral lead to the following expression of $p_{1,r}(t)$

$$p_{1,r}(t) = \int_0^1 \exp(-(r-1)\lambda_t(-\log x)^{1/k_t})\, dx. \tag{6}$$

A key element of our approach is that, for a given year t, record probabilities can be deduced from the Weibull distribution with parameters (k_t, λ_t). Hence, checking the Weibull hypothesis has to be done only once. If not rejected, any $p_{1,r}(t)$ can be inferred for any r. So, our inference strategy is to first infer these two parameters and then plug their estimates in (6). Concerning the first step, it can be implemented by coupling a Nadaraya-Watson kernel regression method with a method of moments to estimate $\hat{\lambda}_t$ and $\hat{k}_t$ (see Section 3 of the Supplementary material and Naveau & Thao, 2022). We call $\widehat{p}_{1,r}(t)$ the estimator obtained by this method. Its theoretical properties can be found in Section 4 of the supplementary material. It is noteworthy that proposition 3 and 5 from Worms & Naveau (2022) states that the parametric estimator based on the Weibull assumption has lower relative error than the non-parametric estimator. Thus, whenever the Weibull assumption can be checked, a parametric approach is preferable for the inference of record probabilities associated to large values of r.

3 Analysis of yearly maxima of daily precipitation

We use our methodology to study annual maxima of daily precipitation, a variable for which the W-class assumption is usually reasonable (see Supplementary material, Section 5). The climate model used here is the IPSL-CM6A-LR from the CMIP6 inter-comparison project. Our factual trajectory of yearly maxima of daily precipitation corresponds to the historical global run over the period 1850 - 2014 combined with the SSP5-8.5 scenario over the period 2015 - 2100. Our counterfactual trajectory is represented by a global run with only natural forcings over the period 1850 – 2020.

To illustrate our approach, we first focus on the analysis of decadal and centennial record probability evolution, i.e. $p_{1,10}(t)$ and $p_{1,100}(t)$ for $t \in \{1850, \ldots, 2100\}$, at a randomly selected grip point near Richmond in Virginia (USA). From Equation (4), we expect to have $\hat{p}_{1,10}(t)$ near 1/10 and $\hat{p}_{1,100}(t)$ near 1/100 during the pre-industrial period. This is confirmed by Figure 3 that displays the decadal (panel (a)) and centennial (panel (b)) record probability estimates of $p_{1,10}(t)$ and $p_{1,100}(t)$ as a function of the year (x-axis). From this grid point near Richmond, a clear climate change signal emerges on decadal records from the year 2002, year from which the confidence interval no longer contains 1/10. By the year 2100, decadal record are almost four times more likely than in a world without climate change.

For the centennial record period, see panel (b), observing a record in 2100 is about ten times more likely than in world without climate change, with a clear climate change signal emerging in 2045. It's noteworthy that this centennial signal emerges more than 40 years later than the signal observed for decadal records. This is due to the fact that the relative error increases as a function of r *(see Proposition 5 from Worms and Naveau, 2022 for details)*. This results in wider confidence intervals and a later detection of a significant signal. This is consistent with our calculations (see Supplementary material, section 4). Smoothing bandwidth is $h = 60.5$ as previously defined by (Naveau & Thao, 2022).

This analysis at a specific location begs the question of when and where a significant attributable signal emerges at the global scale. To answer this question, we leverage Equation (4) and we define record emergence time associated with a given record

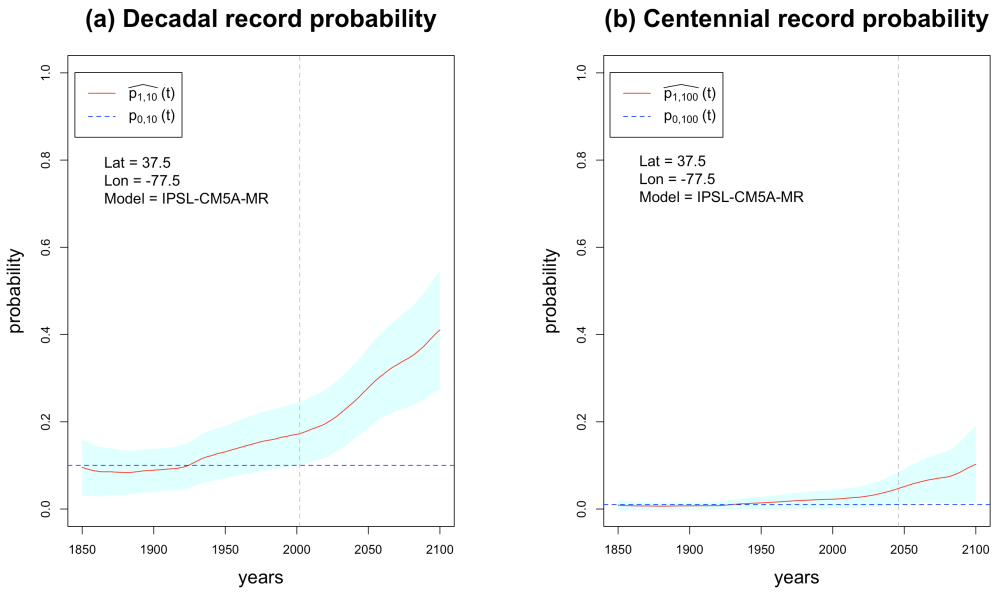

Figure 3. Decadal (a) and centennial (b) record probability of yearly maxima of daily precipitation at Richmond, Virginia grid-point (latitude 37.5, longitude -77.5), using the IPSL-CM6A-LR climate model and the scenario SSP5-8.5, with spatial resolution of 5 x 5 degrees. The light blue zones represent the asymptotic confidence intervals of confidence level 95%.

length r as the first year when $\hat{p}_{1,r}(t)$ is significantly different from its counterfactual value, i.e. different from $p_{0,r}(t) = 1/r$, with confidence level of 95%. Mathematically, this brings the following definition

$$\tau_{0.95}(r) = \min\left\{ t \ \text{ such that for all } t' \geq t, \ \frac{1}{r} \notin [\hat{p}_{1,r}(t') \pm 1.96\, \widehat{\sigma}_{rt'}] \right\}, \tag{7}$$

where $\widehat{\sigma}_{rt}$ represents the estimation of the asymptotic standard deviation and 1.96 corresponds to the Gaussian significance level 0.95 (see Section 4 of the supplementary material for details). Equation (7) allows us to identify the emergence year of any gridpoint. Panel (a) of Figure 4 highlights decadal record probability ratio on 2050 in the zones where by that year there is already a clear signal of climate change. By 2050, there is a clear signal on 80% of the globe, we expect decadal records on tropical latitudes to be up to seven times more likely than in a world without anthropogenic forcing. We do not only observe an increase of decadal record probability, we can also identify a clear decrease in the south and north Atlantic ocean and the south Pacific ocean, which is consistent with previous studies showing a decline of precipitation in these zones (Pfahl et al., 2017). Between these zones of increasing and decreasing probability we observe transition zones, where climate change effect is not clear. When analyzing centennial records, even if climate change signal is less clear, the increase and decrease of probability patterns remain unchanged. Equation (7) also brings out climate change signal timeline. Panel (b) of Figure 4 shows decadal record emergence times, i.e. $\tau_{0.95}(10)$ over the globe. 26% of climate change signal emerged between 2000 and 2023, adding up to this last year 57% of the globe. An equivalent analysis for centennial records can be found in section 6 of the supplementary material.

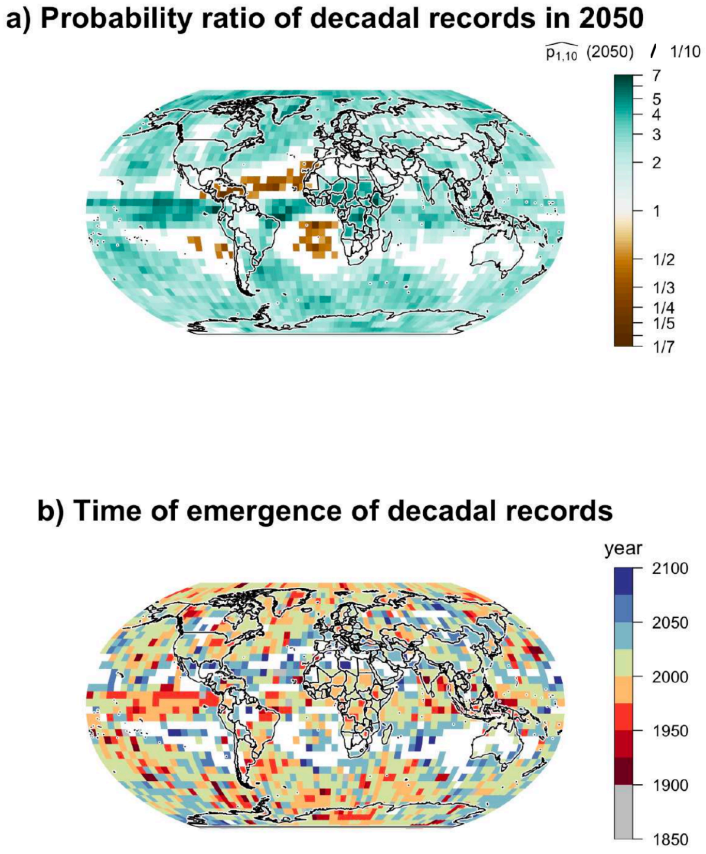

Figure 4. (a) Decadal record probability ratio on 2050 with respect to the counterfactual world, the white zones represent the gridpoints where by 2050 climate change signal has still not emerged, using (7) as criteria. (b) Emergence record times defined by (7), the white zones represent the gridpoints where by 2100 climate change signal has still not emerged, the grey points represent the gridpoints where $\hat{p}_{1,10}(t)$'s confidence interval does not contains 1/10 during the pre-industrial period, these points are left out of our analysis as considered poorly represented. Results obtained using the IPSL-CM6A-LR climate model and the scenario SSP5-8.5, with a spatial resolution of 72 x 36 grid points.

4 Conclusion and discussion

To summarize, we proposed and studied a new EEA record analysis in a transient setup to estimate record probability at each time step t and for any record length r. Our approach accounts for the non-stationarity of the factual world without constraining the shape parameter of the GEV distributions to be constant. This represents an added value compared to methods based on return periods where non-stationarity is not fully captured. Additionnaly, it fills a methodological gap for record analysis, as records have usually been studied in a stationary context, with limited advances on non-stationary times series. Furthermore, our approach has a straightforward interpretation and it bypasses

the separate estimation of both distributions X_t and Z_t separately. By focusing on relative changes between the counterfactual and factual worlds (see Equation (1) of (Naveau & Thao, 2022), we mitigate the underestimation bias of climate models on the climate change signal associated with extreme precipitation (Min et al., 2011; Fischer & Knutti, 2015). In our framework $(X_1, ..., X_t)$ are considered independent. Yet, our approach is still valid in a dependent scenario, if the sequence corresponds to any max-stable time series.

Our analysis of yearly maxima of daily precipitation obtained from the IPSL-CM6A-LR (scenario SSP5-8.5) indicates that precipitation records are affected all over the world, with a clear climate change signal on decadal records before the year 2050. The tropical latitudes and the polar circles appear to be the zones where record probabilities will increase the most and the north and south Atlantic ocean those where they clearly decrease. This result is consistent with previous studies on changes of precipitation (Pfahl et al., 2017; Tandon et al., 2018; Dong et al., 2021). However, our conclusions are only valid for the IPSL-CM6A-LR climate model. As improvements of this methodology, it would be interesting to incorporate multi-model climate error. For example, the technique proposed by Naveau and Thao (2022) may be used to handle this type of error. In addition, our analysis was made independently for each grid and it is likely that the signal in record emergence times will be enhanced by incorporating spatial information at a regional scale. Although more statistically complex, multivariate EVT used in EEA (Kiriliouk & Naveau, 2020) could be implemented to perform this task.

Acknowledgments

Part of this work was supported by the French national program (80 PRIME CNRS-INSU), and the European H2020 XAIDA (Grant agreement ID: 101003469). This work benefited from state aid managed by the National Research Agency under France 2030 bearing the reference ANR-22-EXTR-0005 (TRACCS-PC4-EXTENDING project). The authors also acknowledge the support of the French Agence Nationale de la Recherche (ANR) under reference ANR-20-CE40-0025-01 (T-REX), and the ANR EXSTA.

Open Research

The simulations of the IPSL-CM6A-LR model used in this paper come from the CMIP6 inter-comparison project (Boucher et al., 2021). They are available through the Earth System Grid Federation. An overview of the guidelines for CMIP6 Data users is available through the Program for Climate Model Diagnosis & Intercomparison (Eyring et al., 2016). The presented methodology was implement using R. Figures were made using R. The code developed in this work is available on GitHub `https://github.com/PaulaFlorencia/A-statistical-method-to-model-non-stationarity-in-precipitation-records-changes`

References

Alexander, L. V. (2016). Global observed long-term changes in temperature and precipitation extremes: A review of progress and limitations in IPCC assessments and beyond. *Weather and Climate Extremes*, *11*, 4–16. doi: https://doi.org/10.1016/j.wace.2015.10.007

Angélil, O., Dáithí, S., Wehner, M., Paciorek, C. J., Krishnan, H., & Collins, W. (2017). An independent assessment of anthropogenic attribution statements for recent extreme temperature and rainfall events. *Journal of Climate*, 5-16. doi: https://doi.org/10.1175/JCLI-D-16-0077.1

Beirlant, J., Goegebeur, Y., Teugels, J., & Segers, J. (2005). *Statistics of Extremes: Theory and Applications*. doi: https://doi.org/10.1002/0470012382

Boucher, O., Denvil, S., Levavasseur, G., Cozic, A., Caubel, A., Foujols, M.-A., ... Marchand, M. (2021). *IPSL IPSL-CM5A2-INCA model output prepared for cmip6 AerChemMIP*. Earth System Grid Federation [Dataset]. doi: https://doi.org/10.22033/ESGF/CMIP6.13641

Chow, Y. S., & Teicher, H. (2003). *Probability Theory: Independence, Interchangeability, Martingales*. New York: Springer New York. doi: https://doi.org/10.1007/978-1-4612-1950-7

Coles, S. (2001). *An Introduction to Statistical Modeling of Extreme Values*. London: Springer. doi: https://doi.org/10.1007/978-1-4471-3675-0

Dong, S., Sun, Y., Li, C., Zhang, X., Min, S.-K., & Kim, Y.-H. (2021). Attribution of Extreme Precipitation with Updated Observations and CMIP6 Simulations. *Journal of Climate*, *34*, 871–881. doi: https://doi.org/10.1175/JCLI-D-19-1017.1

Eyring, V., Bony, S., Meehl, G. A., Senior, C. A., Stevens, B., Stouffer, R. J., & Taylor, K. E. (2016). *Overview of the coupled model intercomparison project phase 6 (cmip6) experimental design and organization* [dataset]. Geoscientific Model Development. Retrieved from `https://gmd.copernicus.org/articles/9/1937/2016/` doi: https://doi.org/10.5194/gmd-9-1937-2016

Fischer, E. M., & Knutti, R. (2015, June). Anthropogenic contribution to global occurrence of heavy-precipitation and high-temperature extremes. *Nature Climate Change*, *5*(6), 560–564. doi: https://doi.org/10.1038/nclimate2617

Gulev, S. K., Thorne, P. W., Ahn, J., Dentener, F. J., Domingues, C. M., Gerland, S., ... Vose, R. S. (2021). Changing state of the climate system [Book Section]. In V. Masson-Delmotte et al. (Eds.), *Climate change 2021: The physical science basis. contribution of working group i to the sixth assessment report of the intergovernmental panel on climate change* (chap. 2). Cambridge, United Kingdom and New York, NY, USA: Cambridge University Press.

Hannart, A., & Naveau, P. (2018). Probabilities of causation of climate changes. *Journal of Climate*, *31*, 5507–5524. doi: https://doi.org/10.1175/JCLI-D-17-0304.1

Hannart, A., Pearl, J., Otto, F. E. L., Naveau, P., & Ghil, M. (2016). Counterfactual causality theory for the attribution of weather and climate-related events. *Bulletin of the American Meteorological Society*, *97*, 99–110. doi: https://doi.org/10.1175/BAMS-D-14-00034.1

Hegerl, G., & Zwiers, F. (2011). Use of models in detection and attribution of climate change. *Wiley interdisciplinary reviews: climate change*, *2*(4), 570–591. doi: https://doi.org/10.1002/wcc.121

Härdle, W. (1991). *Smoothing techniques : With implementation in s*. Springer-Verlag, New York: Springer Series in Statistics. doi: https://doi.org/10.1007/978-1-4612-4432-5

IPCC. (2014). *Climate change 2014: Mitigation of climate change. contribution of working group III to the fifth assessment report of the intergovernmental panel on climate change* (O. Edenhofer et al., Eds.). Cambridge University Press, Cambridge and New York, NY.

Katz, R. W., Parlange, M. B., & Naveau, P. (2002). Statistics of extremes in hydrology. *Advances in Water Resources*, *25*(8-12), 1287. doi: https://doi.org/10.1016/S0309-1708(02)00056-8

Kiriliouk, A., & Naveau, P. (2020). Climate extreme event attribution using multivariate peaks-over-thresholds modeling and counterfactual theory. *Annals of Applied Statistics*, *14*(3), 1342-1358. doi: https://doi.org/10.1214/20-AOAS1355

Li, C., Zwiers, F., Zhang, X., Li, G., Sun, Y., & Wehner, M. (2021). Changes in annual extremes of daily temperature and precipitation in cmip6 models. *Journal of climate*, ., 3441–3460. doi: https://doi.org/10.1175/JCLI-D-19-1013.1

Min, S.-K., Zhang, X., Zwiers, F. W., & Hegerl, G. C. (2011, February). Human

contribution to more-intense precipitation extremes. *Nature*, *470*(7334), 378–381. doi: https://doi.org/10.1038/nature09763

Naveau, P., Hannart, A., & Ribes, A. (2020). Statistical Methods for Extreme Event Attribution in Climate Science. *Annual Reviews of Statistics and its Application*. doi: https://doi.org/10.1146/annurev-statistics-031219-041314

Naveau, P., Ribes, A., Zwiers, F., Hannart, A., Tuel, A., & Yiou, P. (2018, May). Revising Return Periods for Record Events in a Climate Event Attribution Context. *Journal of Climate*, *31*(9), 3411–3422. doi: https://doi.org/10.1175/JCLI-D-16-0752.1

Naveau, P., & Thao, S. (2022). Multimodel Errors and Emergence Times in Climate Attribution Studies. *Journal of Climate*, *35*(14), 4791–4804. (Publisher: American Meteorological Society Section: Journal of Climate) doi: https://doi.org/10.1175/JCLI-D-21-0332.1

Pfahl, S., O Gorman, P. A., & Fischer, E. M. (2017). Understanding the regional pattern of projected future changes in extreme precipitation. *Nature Climate Change*, *7*, 423–427. doi: https://doi.org/10.1038/nclimate3287

Stott, P. A., Christidis, N., Otto, F. E. L., Sun, Y., Vanderlinden, J., van Oldenborgh, G. J., ... Zwiers, F. W. (2016). Attribution of extreme weather and climate-related events. *WIREs Climate Change*, *7*(1), 23–41. doi: https://doi.org/10.1002/wcc.380

Tandon, N. F., Zhang, X., & Sobel, A. H. (2018). Understanding the Dynamics of Future Changes in Extreme Precipitation Intensity. *Geophysical Research Letters*, *45*, 2870–2878. doi: https://doi.org/10.1002/2017GL076361

Worms, J., & Naveau, P. (2022). Record events attribution in climate studies. *Environmetrics*, *33*(8). doi: https://doi.org/10.1002/env.2777